

2

AD-A242 332



DTIC  
C D

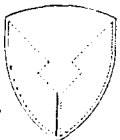
NASA  
Technical  
Paper  
3096

AVSCOM  
Technical  
Report  
91-C-020

August 1991

# A Method for Determining Spiral-Bevel Gear Tooth Geometry for Finite Element Analysis

Robert F. Handschuh  
and Faydor L. Litvin



US ARMY  
AVIATION  
SYSTEMS COMMAND  
AVIATION R&T ACTIVITY

Approved for public release;  
Distribution Unlimited

NASA

91-14967



91 1104 046

**NASA  
Technical  
Paper  
3096**

**AVSCOM  
Technical  
Report  
91-C-020**

1991

# A Method for Determining Spiral-Bevel Gear Tooth Geometry for Finite Element Analysis



Robert F. Handschuh  
*Propulsion Directorate  
U.S. Army-AVSCOM  
Lewis Research Center  
Cleveland, Ohio*

Faydor L. Litvin  
*University of Illinois at Chicago  
Chicago, Illinois*

Accession For	
DTIC GRAFI	<input checked="" type="checkbox"/>
DTIC TAB	<input type="checkbox"/>
Unannounced	<input type="checkbox"/>
Justification	
By _____	
Distribution/	
Availability Codes	
Dist	Avail and/or Special
A-1	

**NASA**

National Aeronautics and  
Space Administration

Office of Management

Scientific and Technical  
Information Program

## Summary

An analytical method has been developed to determine gear-tooth surface coordinates of face-milled spiral bevel gears. The method uses the basic gear design parameters in conjunction with the kinematical aspects of spiral bevel gear manufacturing machinery. A computer program entitled "SURFACE" was developed to calculate the surface coordinates and provide three-dimensional model data that can be used for finite element analysis. Development of the modeling method and an example case are presented in this report. This method of analysis could also be applied in gear inspection and near-net-shape gear forging die design.

## Introduction

Spiral bevel gears are currently used in all helicopter power transmission systems. This type of gear is required to turn the corner from a horizontal engine to the vertical rotor shaft. These gears carry large loads and operate at high rotational speeds. Recent research has focused on understanding many aspects of spiral bevel gear operation, including gear geometry (refs. 1 to 12), gear dynamics (refs. 13 to 15), lubrication (ref. 16), stress analysis and measurement (refs. 17 to 21), misalignment (refs. 22 and 23), and coordinate measurements (refs. 24 and 25), as well as other areas.

Research in gear geometry has concentrated on understanding the meshing action of spiral bevel gears (refs. 8 to 11). This meshing action often results in much vibration and noise due to an inherent lack of conjugation. Vibration studies (ref. 26) have shown that in the frequency spectrum of an entire helicopter transmission, the highest response can be that from the spiral bevel gear mesh. Therefore if noise reduction techniques are to be implemented effectively, the meshing action of spiral bevel gears must be understood.

Also, investigators (refs. 18 and 19) have found that typical design stress indices for spiral bevel gears can be significantly different from those measured experimentally. In addition to making the design process one of trial and error (forcing one to rely on past experience), this inconsistency makes extrapolating over a wide range of sizes difficult, and an overly conservative design can result.

Research has been ongoing in an attempt to predict stresses (i.e., bending and contact) by using the finite element method. A great deal of work (refs. 27 to 30) has gone into finite

element modeling of parallel axis gears to determine the stress field. Loads are typically applied at the point of highest single tooth contact, and then the stress in the fillet region is examined. Computer programs that perform this type of analysis are usually two dimensional in nature and have computer storage requirements that are small enough for personal computers. These attributes make them very popular and attractive to designers. However, a limited number of researchers (refs. 16 and 21) have investigated finite element analysis of spiral bevel gears.

Parallel axis components (involute tooth geometry) have closed-form solutions that determine surface coordinates. These coordinates can be used as input to finite element methods and other analysis tools. Spiral bevel gears, on the other hand, do not have a closed-form solution to describe their surface coordinates. Coordinate locations must be solved numerically. This process is accomplished by modeling the kinematics of the cutting or grinding machinery and the geometry of the basic gear design.

The objective of the research reported herein was to develop a method for calculating spiral bevel gear-tooth surface coordinates and a three-dimensional model for finite element analysis. Accomplishment of this task required a basic understanding of the gear manufacturing process, which is described herein by use of differential geometry techniques (ref. 1). Both the manufacturing machine settings and the basic gear design data were used in a numerical analysis procedure that yielded the tooth surface coordinates. After the tooth surfaces (drive and coast sides) were described, a three-dimensional model for the tooth was assembled. A computer program, SURFACE, was developed to automate the calculation of the tooth surface coordinates, and hence, the coordinates for the gear-tooth three-dimensional finite element model. The development of the analytical model is explained, and an example of the finite element method is presented.

## Determination of Tooth Surface Coordinates

The spiral gear machining process described in this paper is that of the face-milled type. Spiral bevel gears manufactured in this way are used extensively in aerospace power transmissions (i.e., helicopter main/tail rotor transmissions) to transmit power between horizontal gas turbine engines and the vertical rotor

shaft. Because spiral bevel gears can accommodate various shaft orientations, they allow greater freedom for overall aircraft layout.

In the following sections the method of determining gear-tooth surface coordinates will be described. The manufacturing process must first be understood and then analytically described. Equations must be developed that relate machine and workpiece motions and settings with the basic gear design data. The simultaneous solution of these equations must be done numerically since no closed-form solution exists. A description of this procedure follows.

### Gear Manufacture

Spiral bevel gears are manufactured on a machine like the one shown in figure 1. This machine cuts away the material between the concave and convex tooth surfaces of adjacent teeth simultaneously. The machining process is better illustrated in

figure 2. The head cutter (holding the cutting blades or the grinding wheel) rotates about its own axis at the proper cutting speed, independent of the cradle or workpiece rotation. The head cutter is connected to the cradle through an eccentric that allows adjustment of the axial distance between the cutter center and cradle (machine) center, and adjustment of the angular position between the two axes to provide the desired mean spiral angle. The cradle and workpiece are connected through a system of gears and shafts, which controls the ratio of rotational motion between the two (ratio of roll). For cutting, the ratio is constant, but for grinding, it is a variable.

Computer numerical controlled (CNC) versions of the cutting and grinding manufacturing processes are currently being developed. The basic kinematics, however, are still maintained for the generation process; this is accomplished by the CNC machinery duplicating the generating motion through point-to-point control of the machining surface and location of the workpiece.

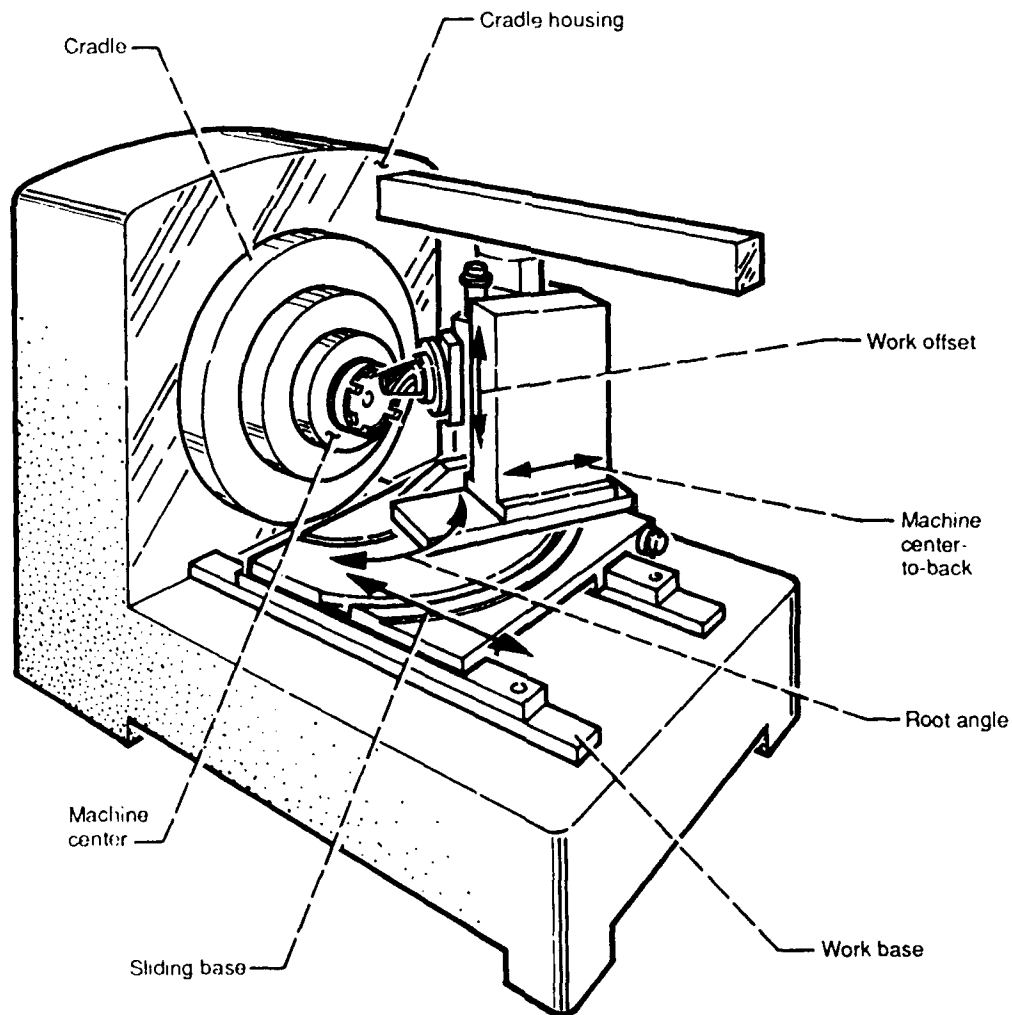


Figure 1. Machine used to generate spiral bevel gear-tooth surface.

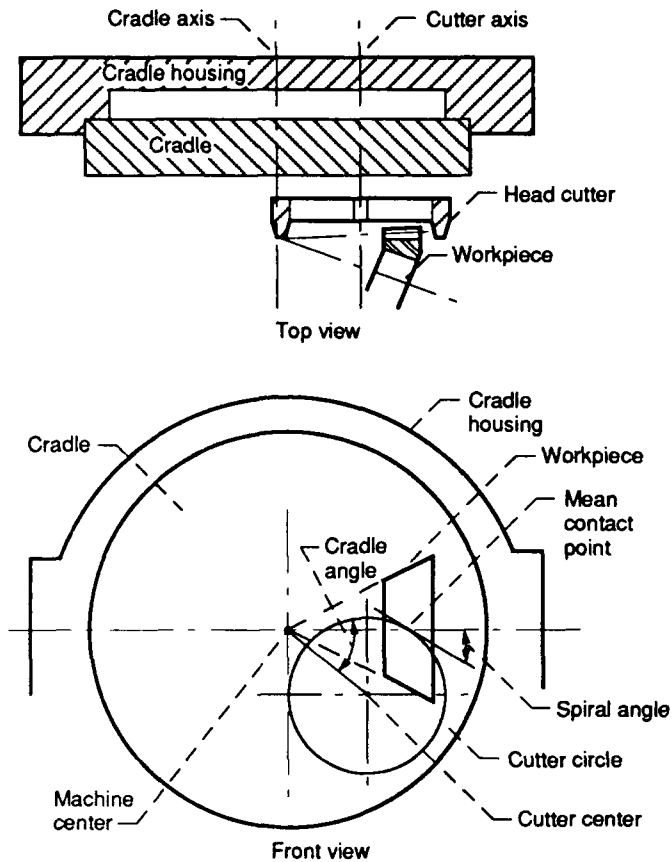


Figure 2.—Orientation of workpiece to generation machinery.

### Coordinate Transformations

The surface of a generated gear is an envelope to the family of surfaces of the head cutter. In simple terms this means that the points on the generated tooth surface are points of tangency to the cutter surface during manufacture. The conditions necessary for envelope existence are given kinematically by the equation of meshing. This equation can be stated as follows: the normal of the generating surface must be perpendicular to the relative velocity between the cutter and the gear-tooth surface at the point in question (ref. 1).

The coordinate transformation procedure that will now be described is required to locate any point from the head cutter into a coordinate system rigidly attached to the gear being manufactured. Homogeneous coordinates are used to allow rotation and translation of vectors simply by multiplying the matrix transformations. The method used for the coordinate transformation can be found in references 1, 5, and 8 to 11.

Let us begin with the head-cutter coordinate system  $S_c$  shown in figure 3. This report assumes that the cutters are straight sided (not curved as commonly used on the wheel for final grinding). Surface coordinates  $u$  and  $\theta$  determine the location of a current point on the cutter surface as well as the orientation of the current point with respect to coordinate system  $S_c$ . Angles  $\psi_{ib}$  and  $\psi_{ob}$  are the inside and outside blade angles. The inside and outside

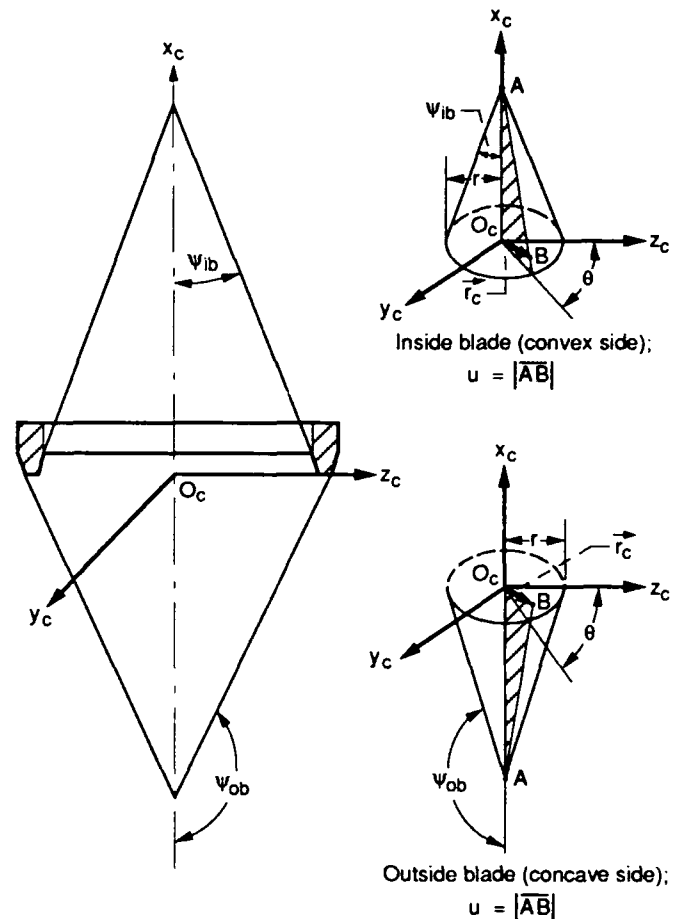


Figure 3.—Head-cutter cone surfaces.

blades cut the convex and concave sides of the gear teeth, respectively. A point on the cutter blade surface is determined by the following:

$$\mathbf{r}_c = \begin{bmatrix} r \cot \psi - u \cos \theta \\ u \sin \psi \sin \theta \\ u \sin \psi \cos \theta \\ 1 \end{bmatrix} \quad (1)$$

where fixed value  $r$  is the radius of the blade at  $x_c = 0$ , and  $\psi$  is the blade angle. Parameters  $u$  and  $\theta$  locate a point in system  $S_c$  and are unknowns whose value will be determined.

The head-cutter coordinate system  $S_c$  is rigidly connected to coordinate system  $S_g$  (fig. 4). System  $S_g$  is rigidly connected to the cradle that rotates about the  $x_m$  axis of the machine coordinate system  $S_m$ . Coordinate system  $S_m$  is a fixed coordinate system and is connected to the machine frame.

To reference the head cutter in coordinate system  $S_c$ , the following transformation is necessary:

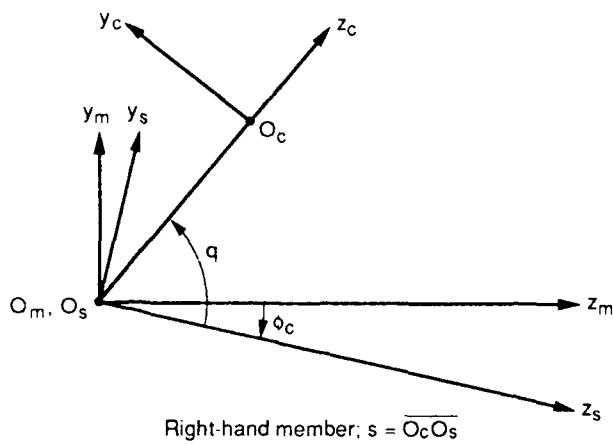
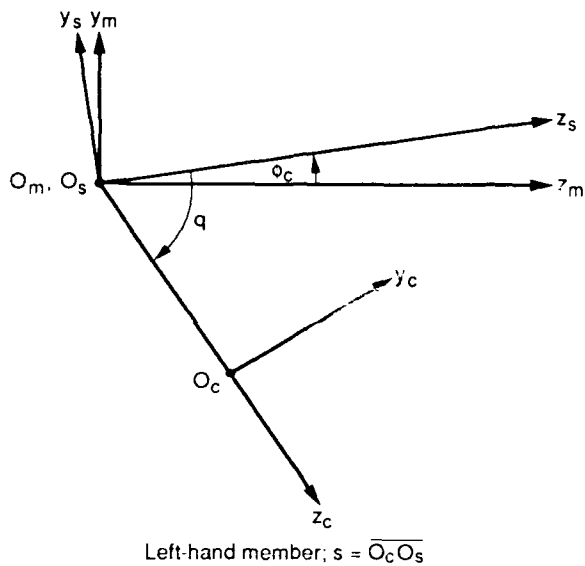


Figure 4.—Orientation of cutter, cradle, and fixed coordinate systems  $S_c$ ,  $S_s$ , and  $S_m$ , respectively.

$$M_{ms} = \begin{bmatrix} 1 & 0 & 0 & 0 \\ 0 & \cos q & \mp \sin q & \mp s \sin q \\ 0 & \pm \sin q & \cos q & s \cos q \\ 0 & 0 & 0 & 1 \end{bmatrix} \quad (2)$$

where  $q$  is the cradle angle and  $s$  is the distance between the Coordinate system  $S_c$  and  $S_s$  origins ( $s = \overline{O_c O_s}$ ). The upper and lower signs preceding the various terms in this matrix transformation (and the rest of the paper) pertain to left- and right-hand gears respectively.

Now, to transform from  $S_c$  to the fixed coordinate system  $S_m$ , the roll angle of the cradle  $\phi_c$  is used. This transformation is given by

$$M_{ms} = \begin{bmatrix} 1 & 0 & 0 & 0 \\ 0 & \cos \phi_c & \pm \sin \phi_c & 0 \\ 0 & \mp \sin \phi_c & \cos \phi_c & 0 \\ 0 & 0 & 0 & 1 \end{bmatrix} \quad (3)$$

Coordinate system  $S_m$  locates the machine center, and coordinate system  $S_p$  orients the pitch apex of the gear being manufactured. The transformation from coordinate system  $S_m$  to coordinate system  $S_p$  requires the machine tool settings  $L_m$  and  $E_m$  along with dedendum angle  $\delta$  from the component design (see figs. 5 and 6). Machine tool settings  $L_m$  and  $E_m$  can be found from the summary sheet that typically accompanies a gear, or the methods in reference 8 can be used. Reference 8 converts standard machine tool settings for the sliding base, the offset, and the machine center-to-back into settings  $L_m$  and  $E_m$ , as shown in table I. The transformation matrix is given by

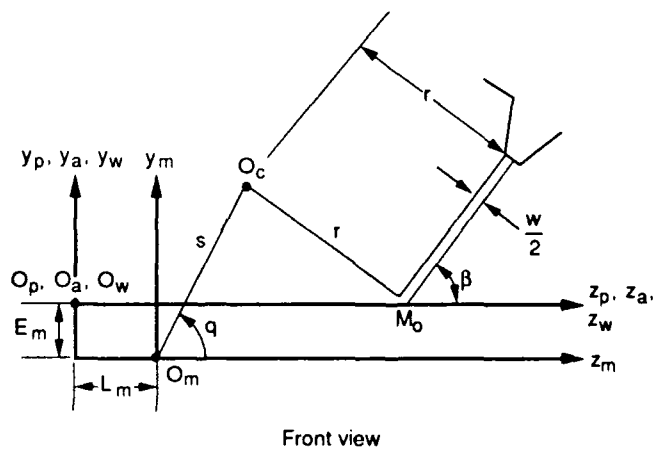
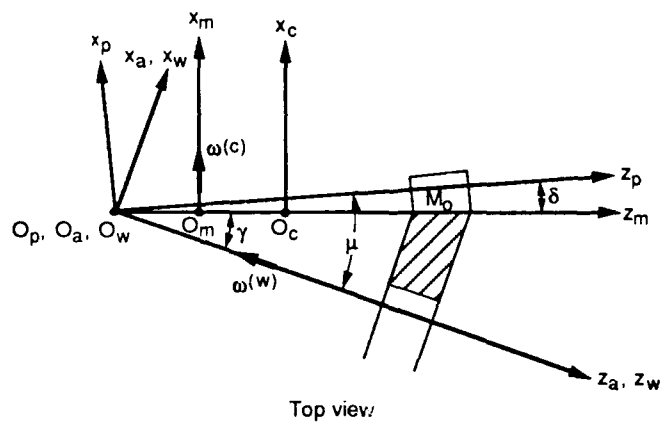
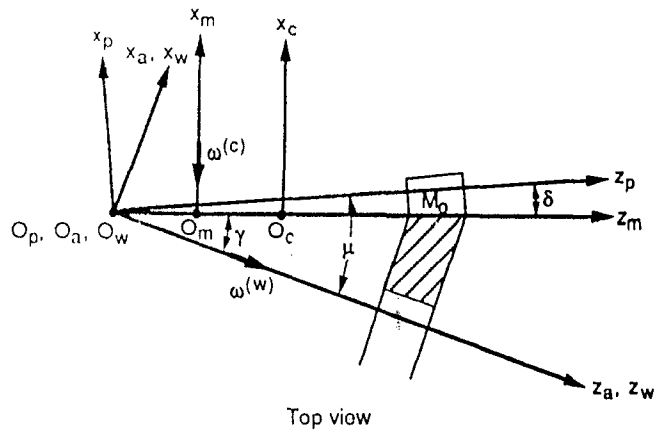


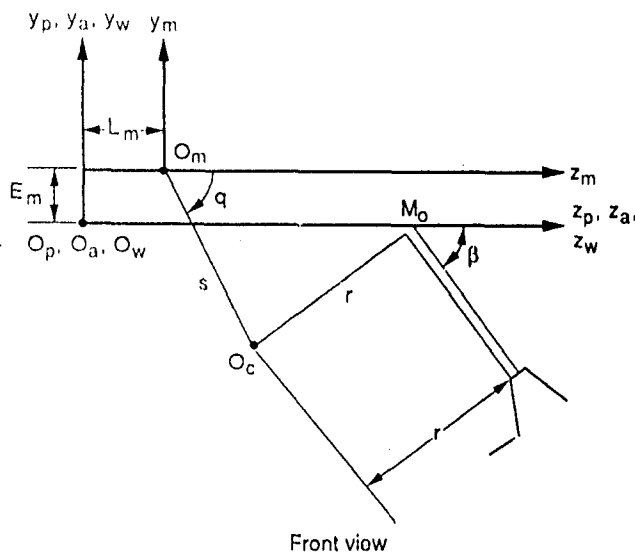
Figure 5.—Coordinate system orientation to generate a right hand gear surface ( $\phi_c = 0$  shown here)



$$M_{pm} = \begin{bmatrix} \cos \delta & 0 & -\sin \delta & -L_m \sin \delta \\ 0 & 1 & 0 & \pm E_m \\ \sin \delta & 0 & \cos \delta & L_m \cos \delta \\ 0 & 0 & 0 & 1 \end{bmatrix} \quad (4)$$

This is shown in figure 5 for a right-hand member and in figure 6 for a left-hand member. Figure 7 is given to clarify the orientation of the coordinate systems and machine tool settings ( $L_m, E_m$ ).

The next transformation involves rotation of system  $S_p$  to  $S_a$ . The common origin for coordinate system  $S_p$  and  $S_a$  locates the apex of the gear under consideration with respect to coordinate system  $S_m$ . This requires rotation about  $y_a$  by the pitch angle  $\mu$  (see fig. 7). This is given by



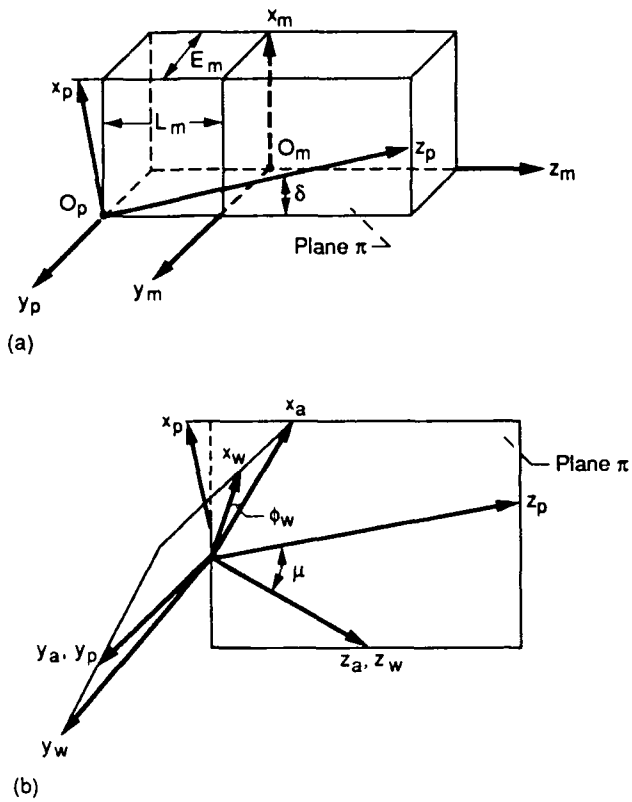
$$M_{ap} = \begin{bmatrix} \cos \mu & 0 & \sin \mu & 0 \\ 0 & 1 & 0 & 0 \\ -\sin \mu & 0 & \cos \mu & 0 \\ 0 & 0 & 0 & 1 \end{bmatrix} \quad (5)$$

The final transformation is from coordinate system  $S_a$  to coordinate system  $S_w$ , which is fixed to the component being manufactured. A rotation about the  $z_p$ -axis through an angle  $\phi_w$  is required. Angle  $\phi_w$ , shown in figure 8, is the workpiece rotation angle; it is directly related to the angle of rotation of the cradle  $\phi_c$  (this relationship will be described in the next section). The  $S_a$  to  $S_w$  coordinate transformation is given by

Figure 6. Coordinate system orientation to generate a left-hand gear surface ( $\phi_w = 0$  shown here).

TABLE I.—SIGN CONVENTIONS OF MACHINE-TOOL SETTINGS  
[From ref. 8.]

Setting	Sign	Right-hand member	Left-hand member
Cradle angle, $q$	+	Counterclockwise (CCW)	Clockwise (CW)
	-	Clockwise (CW)	Counterclockwise (CCW)
Machining offset, $E_m$	+	Above machine center	Below machine center
	-	Below machine center	Above machine center
Machine center-to-back, $X_{MCB}$	+	Work withdrawal	Work withdrawal
	-	Work advance	Work advance
Sliding base, $X_{SB}$	+	Work withdrawal	Work withdrawal
	-	Work advance	Work advance
Vector sum of $X_{SB}$ and $X_{MCB}$	+	$X_{SB} + ; X_{MCB} -$	$X_{SB} + ; X_{MCB} -$
	-	$X_{SB} - ; X_{MCB} +$	$X_{SB} - ; X_{MCB} +$



(a) Machine settings and orientation.  
 (b) Plane  $\pi$  and orientation of generated gear coordinates.

Figure 7.—Orientation of machine settings and generated gear coordinate systems.

$$M_{w,a} = \begin{bmatrix} \cos \phi_w & \pm \sin \phi_w & 0 & 0 \\ \mp \sin \phi_w & \cos \phi_w & 0 & 0 \\ 0 & 0 & 1 & 0 \\ 0 & 0 & 0 & 1 \end{bmatrix} \quad (6)$$

Using these matrix transformations, we can determine the coordinates in  $S_w$  of a point on the generating surface from

$$\mathbf{r}_w = [M_{w,a}][M_{ap}][M_{pm}][M_{ms}][M_{sc}]\mathbf{r}_c \quad (7)$$

or

$$\mathbf{r}_w = [M_{w,a}f(\phi_c)][M_{ap}][M_{pm}][M_{ms}(\phi_c)][M_{sc}]\mathbf{r}_c(u, \theta) \quad (8)$$

or

$$\mathbf{r}_w = \mathbf{r}_w(u, \theta, \phi_c) \quad (9)$$

This transformation describes the location of a point in the gear fixed coordinate system based on machine settings ( $L_m$ ,  $E_m$ ,  $q$ ,  $s$ ,  $r$ , and  $\psi$ ), parameters ( $u$ ,  $\theta$ , and  $\phi_c$ ), and gear design information ( $\mu$  and  $\delta$ ).

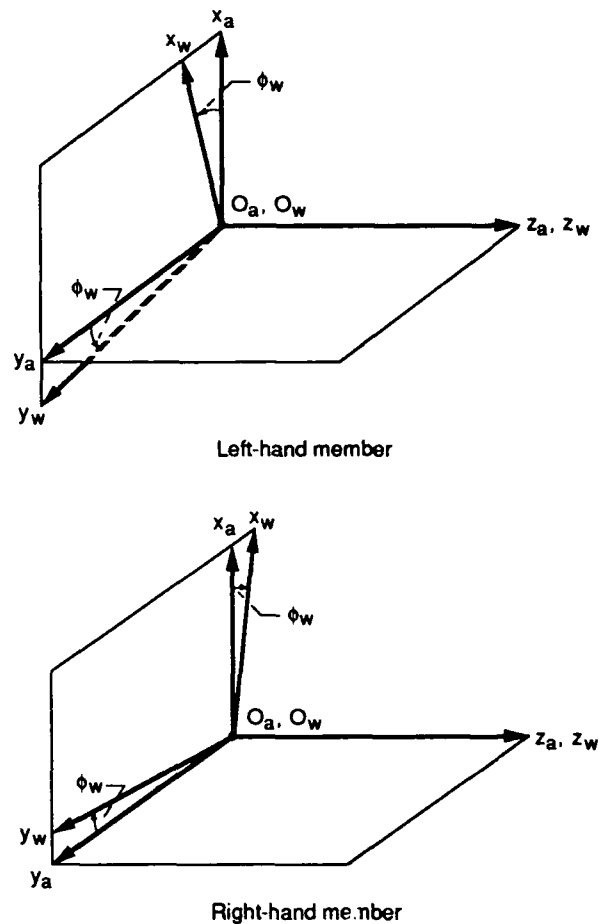


Figure 8.—Rotation of workpiece for left- and right-hand gears during tooth-surface generation.

### Tooth Surface Coordinate Solution Procedure

In order to solve for the coordinates of a spiral bevel gear-tooth surface, the following items must be used simultaneously: the transformation process, the equation of meshing, and the basic gear design information. The transformation process described previously is used to determine the location of a point on the head cutter in coordinate system  $S_w$ . Since there are three unknown quantities ( $u$ ,  $\theta$ , and  $\phi_c$ ), three equations relating them must be developed.

Values for  $u$ ,  $\theta$ , and  $\phi_c$  are used to satisfy the equation of meshing given by references 1 and 9:

$$\mathbf{n} \cdot \mathbf{V} = 0 \quad (10)$$

where  $\mathbf{n}$  is the normal vector to the cutter and workpiece surfaces at the specified location of interest, and  $\mathbf{V}$  is the relative velocity between the cutter and workpiece surfaces at the specified location. From the reference 9 equation of meshing for straight-sided cutters with a constant ratio of roll between the cutter and workpiece, equation (10) is defined as

$$\begin{aligned}
& (u - r \cot \psi \cos \psi) \cos \gamma \sin \tau \\
& + s[(m_{cu} - \sin \gamma) \cos \psi \sin \theta \mp \cos \gamma \sin \psi \sin (q - \phi_c)] \\
& \pm E_m (\cos \gamma \sin \psi + \sin \gamma \cos \psi \cos \tau) \\
& - L_m \sin \gamma \cos \psi \sin \tau = 0 \quad (11)
\end{aligned}$$

where  $\gamma$  is the root angle of the component being manufactured, and

$$\tau = (\theta \mp q \pm \phi_c) \quad (12)$$

and

$$m_{cu} = \frac{\omega^{(c)}}{\omega^{(w)}} \quad (13)$$

where  $m_{cu}$  is the ratio of angular velocity of the cradle to that of the workpiece. Since the ratio of roll in this report is assumed to be constant, equation (13) can be written as

$$\omega^{(w)} = \frac{\omega^{(c)}}{m_{cu}}$$

and

$$\omega^{(w)} = \frac{d\phi_w}{dt}; \quad \omega^{(c)} = \frac{d\phi_c}{dt}$$

therefore

$$\int \phi_w dt = \frac{1}{m_{cu}} \int \phi_c dt$$

or

$$\phi_w = \frac{\phi_c}{m_{cu}} \quad (14)$$

Equation (14) is the relationship between the cradle and workpiece for a constant ratio of roll and is used directly in equation (6).

Gear design information is then used to establish an allowable range of values of the radial ( $r$ ) and axial ( $z$ ) positions that are known to exist on the gear being generated. This is shown in figure 9.

First the equation of meshing must be satisfied. This was shown earlier to be

$$\mathbf{n} \cdot \mathbf{V} = 0$$

or

$$f_1(u, \theta, \phi_c) = 0 \quad (15)$$

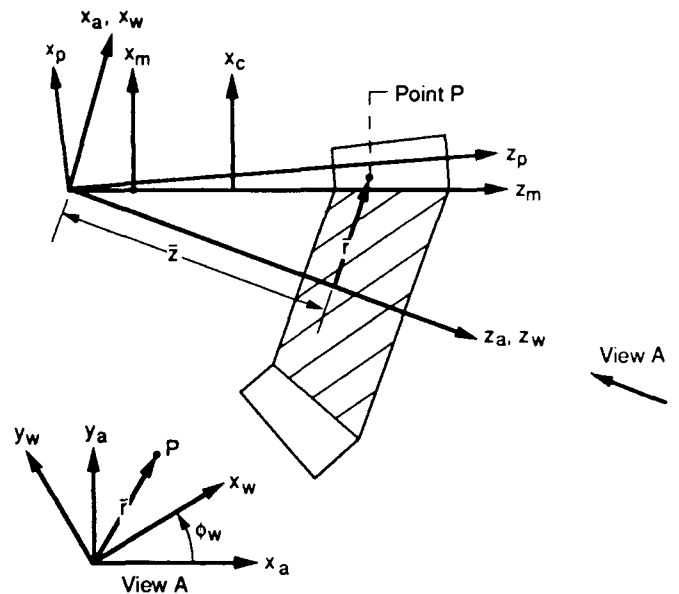


Figure 9.—Orientation of gear to be generated, with assumed positions  $r$  and  $z$ .

The axial position must match the value found from transforming the cutter coordinates  $S_c$  to workpiece coordinates  $S_w$ . This is satisfied by the following (fig. 9):

$$z_w - z = 0 \quad (16)$$

or

$$f_2(u, \theta, \phi_c) = 0 \quad (17)$$

Finally the radial location from the work axis of rotation must be satisfied. This is accomplished by using the magnitude of the location in question in the  $x_w$ - $y_w$  plane (see fig. 9):

$$r - (x_w^2 + y_w^2)^{0.5} = 0 \quad (18)$$

or

$$f_3(u, \theta, \phi_c) = 0 \quad (19)$$

Now a system of three equations (eqs. (15), (17), and (19)) is solved simultaneously for the three parameters  $u$ ,  $\theta$ , and  $\phi_c$ , for a given gear design with a set of machine tool settings. These are nonlinear algebraic equations that can be solved numerically with commercially available mathematical subroutines. These equations are then solved simultaneously for each location of interest along the tooth flank, as shown in figure 10. In the SURFACE program a 10 by 10 grid of points is used on each side of the tooth. From the surface grids, the active profile (working depth) occupied by a single tooth is defined.

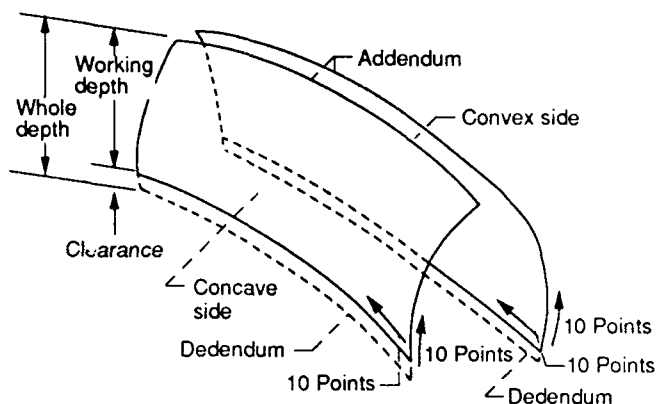


Figure 10.—Calculation points (10 by 10 grids, i.e., 100 points each side) for concave and convex sides of tooth surface.

## Application of Solution Technique

An application of the techniques previously discussed will now be presented. The component to be modeled was from the NASA Lewis Spiral Bevel Gear Test Facility. A photograph of the spiral bevel gear mesh is shown in figure 11, and the design data for the pinion member are shown in table II.

The gear design data were used along with the methods of reference 9 to determine the machine tool settings for straight-sided cutters (see table II). These values were then used as input to SURFACE. This program calculates the coordinates



C-77-117

Figure 11.—NASA spiral bevel gear test rig components.

of the concave and convex sides of the gear tooth (fig. 10), orients the surfaces such that the top land is of the proper width, and then generates the required data for the three-

TABLE II.—EXAMPLE CASE OF SURFACE COORDINATE GENERATION  
(a) Pinion design data

Number of teeth		
pinion.....		12
gear.....		36
Dedendum angle, deg.....		1.0
Addendum angle, deg.....		3.883
Pitch angle, deg.....		18.433
Shaft angle, deg.....		96.0
Mean spiral angle, deg.....		35.0
Face width, mm (in.).....		25.4 (1.0)
Mean cone distance, mm (in.).....		81.05 (3.191)
Inside radius of gear blank, mm (in.).....		15.3 (0.6094)
Top land thickness, mm (in.).....		2.032 (0.080)
Clearance, mm (in.).....		0.762 (0.030)

(b) Generation machine settings

	Concave	Convex
Radius of cutter, $r$ , mm (in.)	75.222 (2.9615)	78.1329 (3.0761)
Blade angle, $\psi$ , deg	161.358	24.932
Vector sum, $L_m$ , mm (in.)	1.0363 (0.0408)	-1.4249 (-0.0561)
Machine offset, $E_m$ , mm (in.)	3.9802 (0.1567)	-4.4856 (-0.1766)
Cradle to cutter distance, $s$ , mm (in.)	74.839 (2.9646)	71.247 (2.8050)
Cradle angle, $q$ , deg	64.01	53.82
Ratio of roll, $m_{r0}$	0.308462	0.321767
Initial cutter length, $u$ , mm (in.)	239.5 (9.43)	181.1 (7.13)
Initial cutter orientation, $\theta$ , deg	120.0	120.0
Initial cradle orientation, $\phi_c$ , deg	0.0	0.0

dimensional modeling program PATRAN (ref. 31). The details of the procedure are described in the following paragraphs.

### Surface Coordinate Calculation

Using figures 10 and 12 as references, we will describe the calculation procedure for surface coordinates. First, the concave side of the tooth is completely defined before moving to the convex side. These points are calculated by starting at the toe end and at the lowest point of active profile. Nine steps of equal distance are used from the beginning of the active profile to the face angle (addendum) of the gear tooth, and then back to the next axial position (see fig. 12). The procedure is repeated until the concave side is completely described. Then the same procedure is followed for the convex side.

In the discussion of surface coordinate determination, the cutting blades were described as straight sided. The point radius  $r$  (eq. (1)) is the radius the cutter would have if it were projected down to the  $y-z$  plane (figs. 3, 5, and 6). Actually, the blade has a theoretical point width and corner radii that generate the portion of the tooth from the working depth to the root cone (see fig. 13). In the section Coordinate Transformations, this part of the cutting blade was not modeled, so the current analysis by SURFACE either assumes a full fillet radius between the lowest point of active profile on adjacent teeth or sets the fillet radius equal to the clearance (fig. 14).

### Concave and Convex Orientation

Since both sides of the gear-tooth surface are not analyzed simultaneously, for proper alignment of the surfaces, their orientation relative to each other must be established by determining the amount of rotation in the fixed coordinate

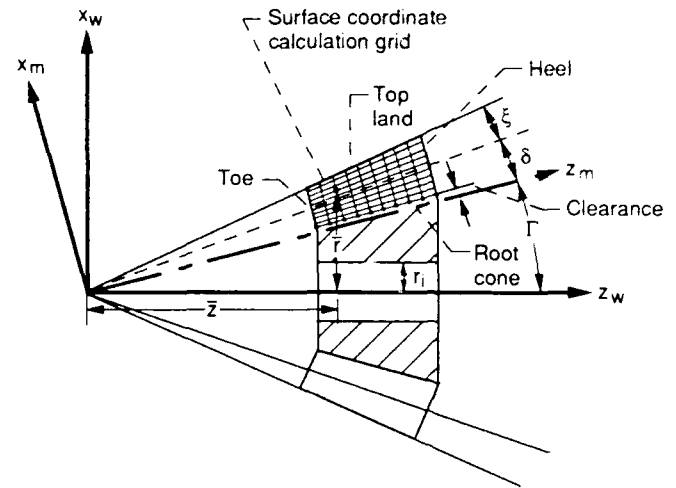


Figure 12. Cross section of calculation grid:  $\gamma$ , root angle;  $\delta$ , dedendum angle;  $\xi$ , addendum angle;  $r_i$ , inside radius of gear blank

system  $S_w$ . This is done by checking the tooth thickness at the face angle on the toe end of the gear tooth. (Also, in the case of a gear, remember that a given cutting operation using cutters as shown in fig. 3 actually cuts adjacent teeth on the convex and concave sides simultaneously.) The distance between these two locations must correspond to the top land width. The convex surface is then rotated according to the angle determined by the points at the face angle at the toe position. This is shown in figure 15. (Note that this same procedure could have been done by considering the tooth mean circular thickness instead of the tooth thickness at the face angle as was done in this report.)

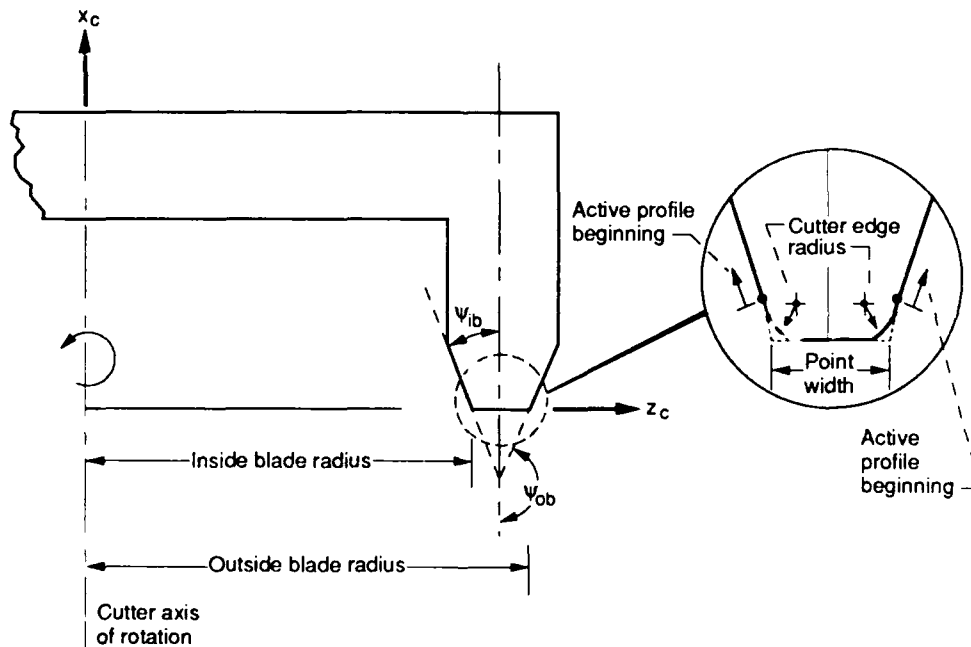


Figure 13. Detailed view of straight sided cutter geometry

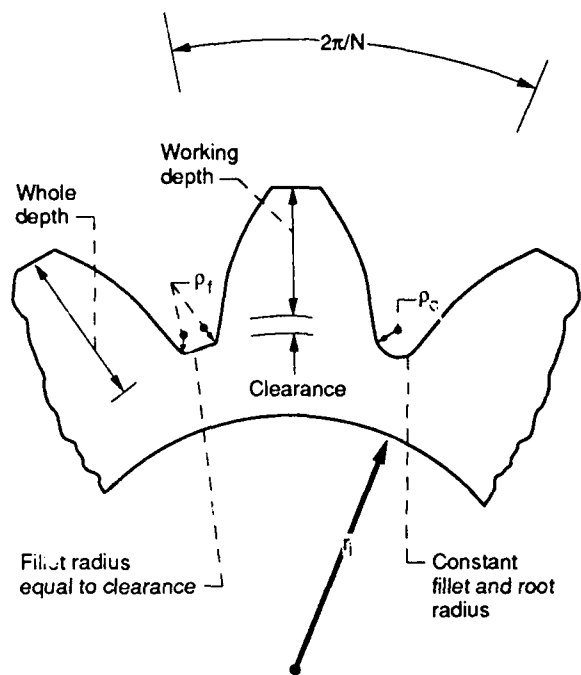


Figure 14.—Two types of fillet and root radius regions used by SURFACE program:  $\rho_c$ , constant fillet and root radius;  $\rho_f$ , fillet radius equal to the clearance;  $N$ , number of teeth;  $r_i$ , inside radius of gear blank.

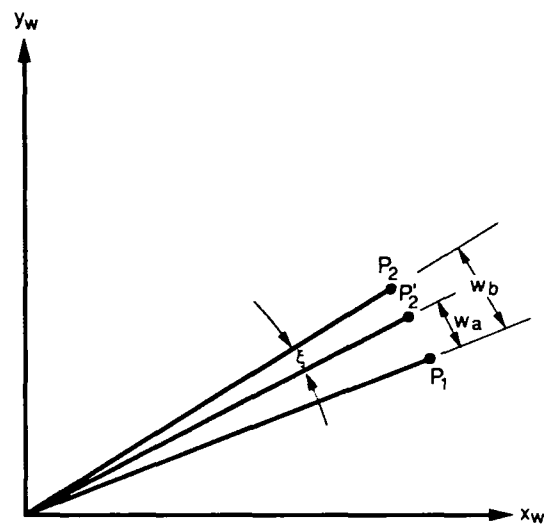


Figure 15.—Orientation of concave and convex sides of gear-tooth surfaces to attain proper top level width by rotation of convex side of tooth:  $P_1$ , concave side location of face angle point at toe end of tooth;  $P_2$  and  $P_2'$ , initial and final convex side locations, respectively, of face angle point at toe end of tooth;  $\xi$ , angle through which  $P_2$  is rotated; and  $w_b$  and  $w_a$ , desired and initial top level thicknesses, respectively.

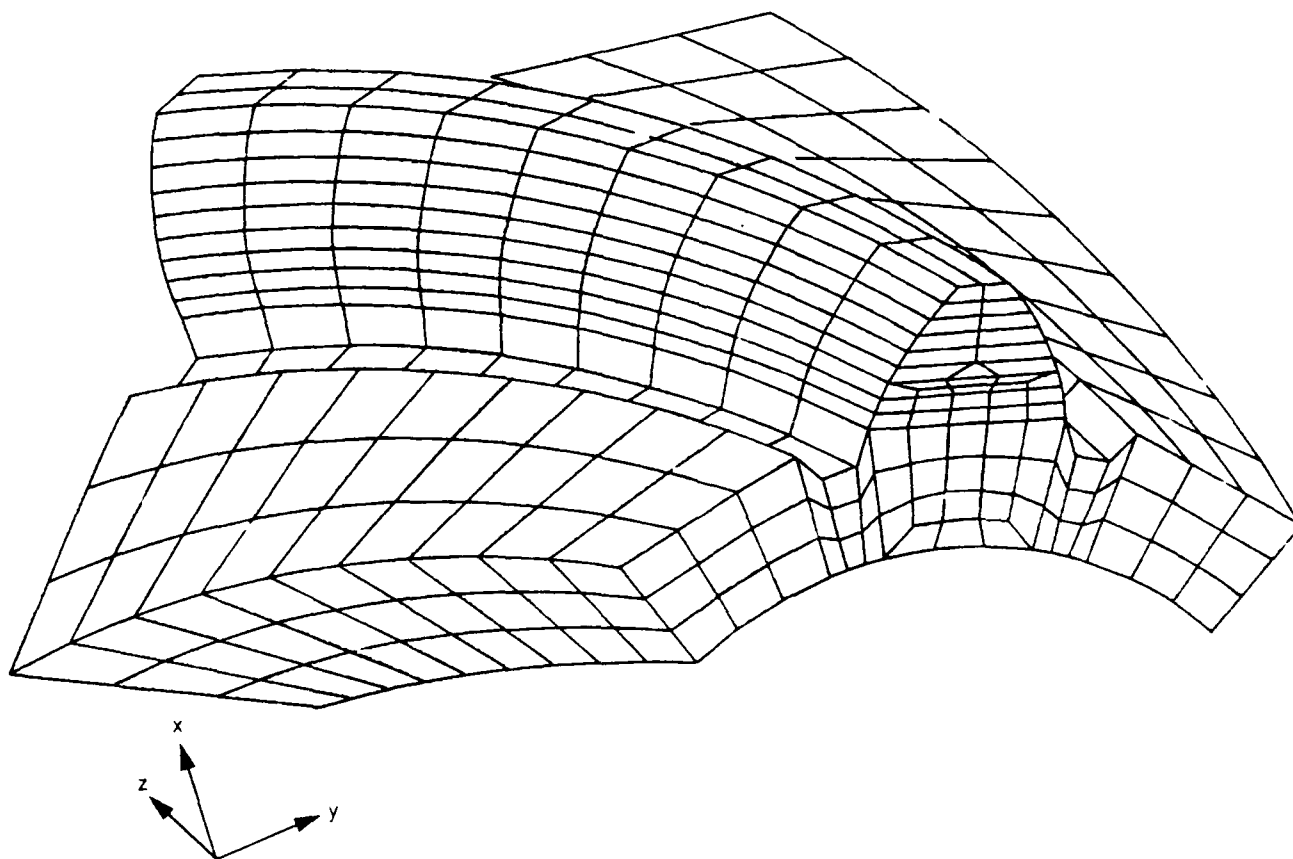


Figure 16.—Hidden line plot of one-tooth model generated by the SURFACE program using PATRAN (constant fillet and root radius model)

## Generation of Three-Dimensional Model Data

Once the surface coordinates are described and properly oriented, then the data necessary for PATRAN have been produced. Currently, the model in SURFACE can have two different fillet and root radii configurations. The fillet radius can be constant at the cross section between adjacent teeth or be equal to the clearance with a flat between the fillet radii of the adjacent teeth at the root angle. Also a constant inside radius of the gear blank is used in this modeling method. These assumptions are depicted in figure 14.

At this point, we have produced a one-tooth model for use in PATRAN. Now, the analyst must determine how complex the model need be for a given application. If a complete gear is required, simply rotate the one-tooth model in PATRAN.

Once the required number of teeth have been described, then the finite element mesh density and the boundary condition information are generated within the PATRAN environment. PATRAN produces the bulk data deck for MSC/NASTRAN and many other computer codes. The example given in this report used MSC/NASTRAN for the static analysis.

## Example Model and Results

From the one-tooth model described earlier the analysis techniques can be demonstrated. The model shown in figure 16 is that for a constant fillet and root radius (called full fillet) model. The fillet and root radius on the convex side has been added along with the tooth section (without the tooth) to make the model symmetric about the tooth centerline. Figure 16 shows a hidden line plot of the finite element mesh with eight-noded isoparametric three-dimensional solid continuum elements. This model has 765 elements and 1120 nodes. The boundary conditions are shown in figure 17. A 1724-MPa (250 ksi) constant pressure load was applied normal to the tooth surface of nine elements, and the two edge surfaces of the gear rim had all degrees of freedom constrained.

The results were calculated by MSC/NASTRAN and were subsequently displayed by PATRAN. Figure 18 shows the principle stresses, and figure 19 shows the total displacements for the boundary conditions shown in figure 17.

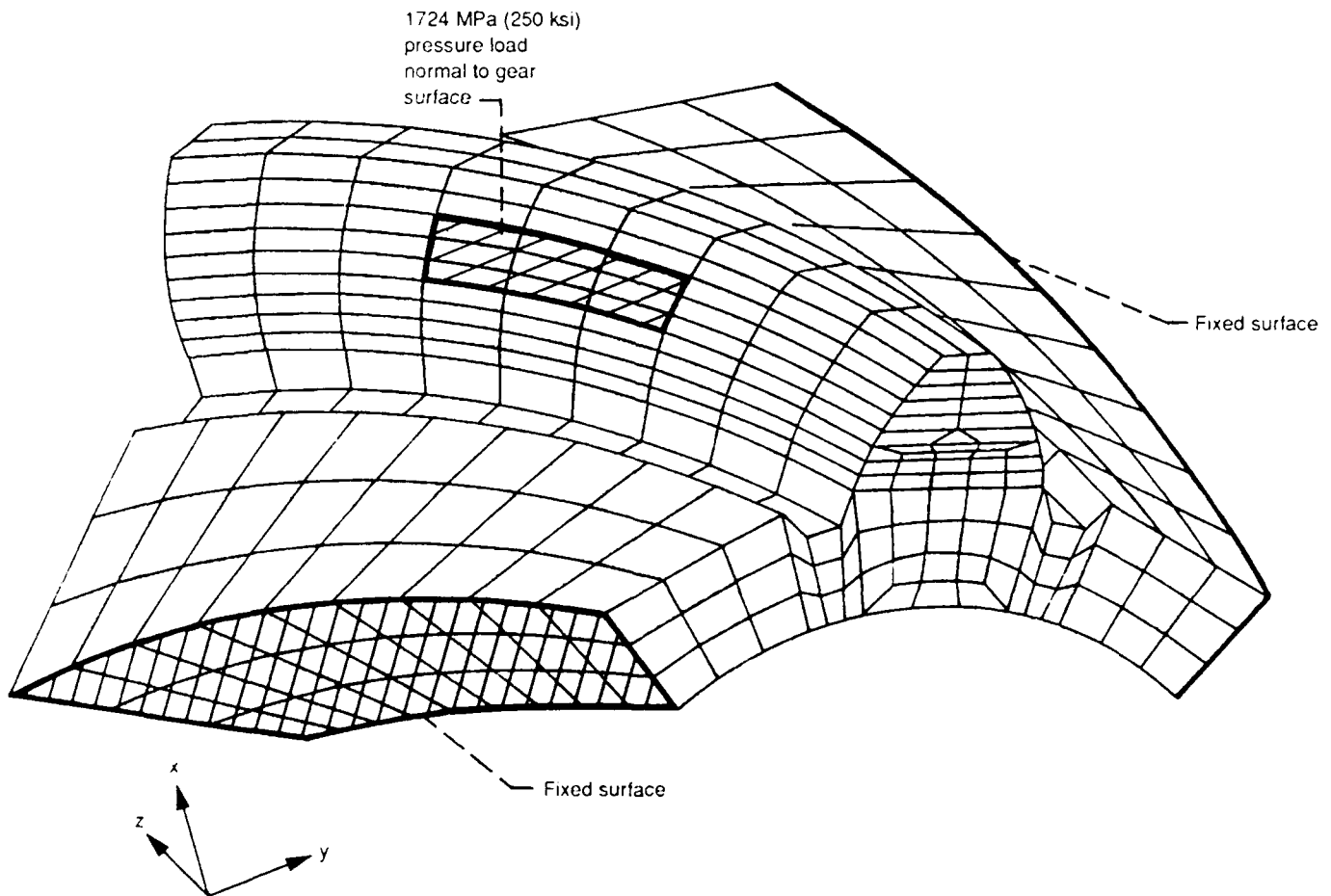


Figure 17. Boundary conditions for constant fillet and root radius model for the example application

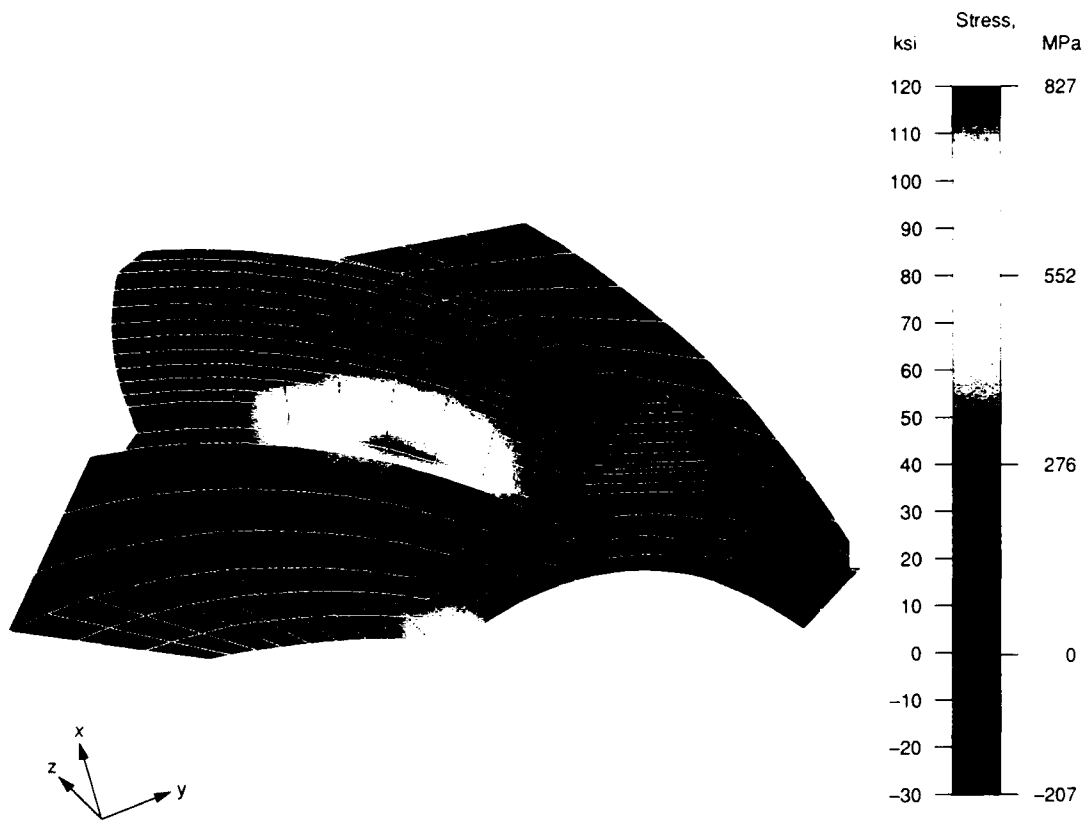


Figure 18.—Major principal stress for boundary conditions specified in figure 17.

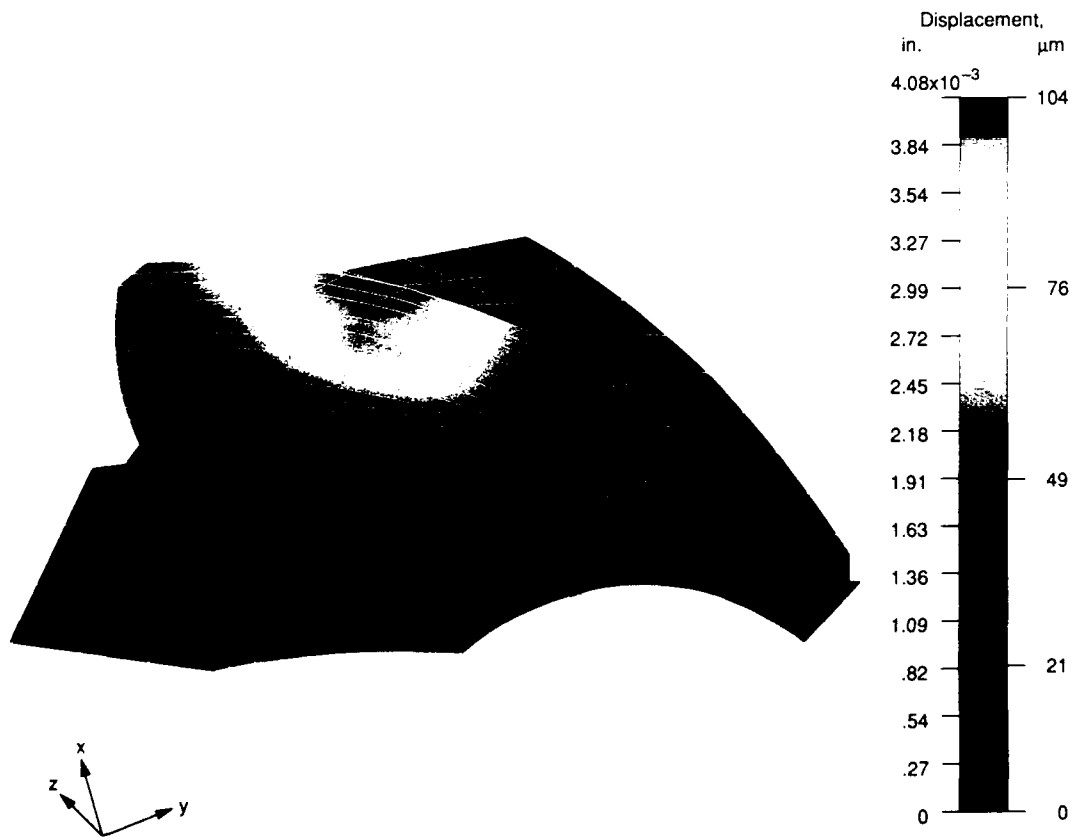


Figure 19.—Total displacement for the boundary conditions specified in figure 17.

## Summary of Results

A method has been presented that uses differential geometry techniques to calculate the surface coordinates of face-milled spiral bevel gear teeth. The coordinates must be solved for numerically by a simultaneous solution of nonlinear algebraic equations. These equations relate the kinematics of manufacture to the gear design parameters. Coordinates for a grid of points are determined for both the concave and convex sides of the gear tooth. These coordinates are then combined to form the enclosed surface of one gear tooth. A computer program, SURFACE, was developed to solve for the gear-tooth surface coordinates and provide input to a three-dimensional geometric modeling program (i.e., PATRAN). This enables an analysis by the finite element method. An example of the technique was presented.

Lewis Research Center  
National Aeronautics and Space Administration  
Cleveland, Ohio, December 19, 1990

## References

1. Litvin, F.L.: Theory of Gearing. NASA RP 1212, 1989.
2. Litvin, F., and Coy, J.: Spiral Bevel Geometry and Gear Train Precision. Advanced Power Transmission Technology, NASA CP-2210, AVRADCOM TR 82-C 16, G.K. Fischer, ed., 1981, pp. 335-344.
3. Huston, R., and Coy, J.: A Basis for the Analysis of Surface Geometry of Spiral Bevel Gears. Advanced Power Transmission Technology, NASA CP-2210, AVRADCOM TR 82-C 16, G.K. Fischer, ed., 1981, pp. 317-334.
4. Chang, S.H.; Huston, R.L.; and Coy, J.J.: Computer Aided Design of Bevel Gear Tooth Surfaces. Proceedings of the 1989 International Power Transmission and Gearing Conference, 5th, Vol. 2, ASME, 1989, pp. 585-591.
5. Litvin, F.L., et al.: Method for Generation of Spiral Bevel Gears With Conjugate Gear Tooth Surfaces. J. Mech. Trans. Automat. Des., vol. 109, no. 2, June 1987, pp. 163-170.
6. Tsai, Y.C.; and Chin, P.C.: Surface Geometry of Straight and Spiral Bevel Gears. J. Mech. Trans. Automat. Des., vol. 109, no. 4, Dec. 1987, pp. 443-449.
7. Cloutier, L.; and Gosselin, C.: Kinematic Analysis of Bevel Gears. ASME Paper 84-DET-177, Oct. 1984.
8. Litvin, F.L.; Tsung, W.J.; and Lee, H.T.: Generation of Spiral Bevel Gears With Conjugate Tooth Surfaces and Tooth Contact Analysis. NASA CR 4088, AVSCOM TR 87-C 22, 1987.
9. Litvin, F.L., and Lee, H.T.: Generation and Tooth Contact Analysis of Spiral Bevel Gears With Predesigned Parabolic Functions of Transmission Errors. NASA CR 4259, AVSCOM TR 89-C 014, 1989.
10. Litvin, F.L., et al.: Transmission Errors and Bearing Contact of Spur, Helical and Spiral Bevel Gears. SAE Paper 881294, Sept. 1988.
11. Litvin, F.L., et al.: New Generation Methods for Spur, Helical, and Spiral Bevel Gears. NASA TM 88862, AVSCOM TR 86-C 27, 1986.
12. Exact Determination of Tooth Surfaces for Spiral Bevel and Hypoid Gears. Gleason Works, Rochester, NY, Aug. 1970.
13. Mark, W.D.: Analysis of the Vibratory Excitation Arising From Spiral Bevel Gears. NASA CR 4081, 1987.
14. Kehrman, A., et al.: Dynamic Analysis of Geared Rotors by Finite Elements. Proceedings of the 1989 International Power Transmission and Gearing Conference, 5th, Vol. 1, ASME, 1989, pp. 375-382.
15. Drago, R.; and Margasabayam, R.: Analysis of the Resonant Response of Helicopter Gears With the 3-D Finite Element Method. Presented at the 1988 MSC/NASTRAN World User's Conference, Mar. 1988.
16. Chao, H.C.; Baxter, M.; and Cheng, H.S.: A Computer Solution for the Dynamic Load, Lubricant Film Thickness, and Surface Temperatures in Spiral Bevel Gears. Advanced Power Transmission Technology, NASA CP 2210, AVRADCOM TR 82-C 16, G.K. Fischer, ed., 1981, pp. 345-364.
17. Winter, H.; and Paul, M.: Influence of Relative Displacements Between Pinion and Gear on Tooth Root Stresses of Spiral Bevel Gears. J. Mech. Trans. Automat. Des., vol. 107, no. 1, Mar. 1985, pp. 43-48.
18. Oswald, F.B.: Gear Tooth Stress Measurements on the UH 60A Helicopter Transmission. NASA TP 2698, 1987.
19. Pizzigati, G.A.; and Drago, R.J.: Some Progress in the Accurate Evaluation of Tooth Root and Fillet Stresses in Lightweight, Thin Rimmed Gears. AGMA Paper 229.21, American Gear Manufacturers Association, Oct. 1980.
20. Wilcox, L.: Analyzing Gear Tooth Stress as a Function of Tooth Contact Pattern Shape and Position. Gear Technology, vol. 2, no. 1, Jan. Feb. 1985, pp. 9-15, 23 (also, AGMA Paper 229.25, 1982).
21. Drago, R.J.; and Uppaluri, B.R.: Large Rotorcraft Transmission Technology Development Program, Vol. 1, Technical Report (D210-11972-1-VOL. 1, Boeing Vertol Co.; NASA Contract NAS3-22143) NASA CR-168116, 1983.
22. Baxter, M.L., Jr.: Effect of Misalignment on Tooth Action of Bevel and Hypoid Gears. ASME Paper 61-MD-20, Mar. 1961.
23. Spear, G.M.; and Baxter, M.L.: Adjustment Characteristics of Spiral Bevel and Hypoid Gears. ASME Paper 66-MECH-17, Oct. 1966.
24. Frint, H.: Automated Inspection and Precision Grinding of Spiral Bevel Gears. NASA CR-4083, AVSCOM TR 87-C 11, 1987.
25. Litvin, F.L., et al.: Computerized Inspection of Gear Tooth Surfaces. NASA TM-102395, AVSCOM TR 89-C 011, 1989.
26. Lewicki, D.G.; and Coy, J.J.: Vibration Characteristics of OH 58A Helicopter Main Rotor Transmission. NASA TP 2705, AVSCOM TR 86-C-42, 1987.
27. Gakwaya, A.; Cardou, A.; and Dhatt, G.: Evaluation of Stresses and Deflection of Spur and Helical Gears by the Boundary Element Method. ASME Paper 84-DET-169, Oct. 1984.
28. Baret, C., et al.: Stress Path Along the Facewidth in Spur Gears Fillet by 3D P-FEM Models. Proceedings of the 1989 International Power Transmission and Gearing Conference, 5th, Vol. 1, ASME, 1989, pp. 173-179.
29. Sun, H., et al.: Comparison of Boundary Element and Finite Element Methods in Spur Gear Root Stress Analysis. Proceedings of the 1989 International Power Transmission and Gearing Conference, 5th, Vol. 1, ASME, 1989, pp. 163-166.
30. Oskul, M.: Three Dimensional Finite Element Stress Predictions of Spur Gears Compared to Gear Fatigue Rig Measurements. AIAA Paper 89-2918, July 1989.
31. PATRAN Users Manual. PDA Engineering, Costa Mesa, CA, July 1987.



National Aeronautics and Space Administration

# Report Documentation Page

1. Report No. NASA TP-3096 AVSCOM TR-91-C-020		2. Government Accession No.		3. Recipient's Catalog No.	
4. Title and Subtitle A Method for Determining Spiral-Bevel Gear Tooth Geometry for Finite Element Analysis				5. Report Date August 1991	
				6. Performing Organization Code	
7. Author(s) Robert F. Handschuh and Faydor L. Litvin				8. Performing Organization Report No. E-5837	
9. Performing Organization Name and Address NASA Lewis Research Center Cleveland, Ohio 44135-3191 and Propulsion Directorate U.S. Army Aviation Systems Command Cleveland, Ohio 44135-3191				10. Work Unit No. 505-63-51 1L162211A47A	
				11. Contract or Grant No.	
12. Sponsoring Agency Name and Address National Aeronautics and Space Administration Washington, D.C. 20546-0001 and U.S. Army Aviation Systems Command St. Louis, Mo. 63120-1798				13. Type of Report and Period Covered Technical Paper	
				14. Sponsoring Agency Code	
15. Supplementary Notes Robert F. Handschuh, Propulsion Directorate, U.S. Army Aviation Systems Command; Faydor L. Litvin, University of Illinois at Chicago, Chicago, Illinois.					
16. Abstract An analytical method has been developed to determine gear-tooth surface coordinates of face-milled spiral bevel gears. The method uses the basic gear design parameters in conjunction with the kinematical aspects of spiral bevel gear manufacturing machinery. A computer program entitled "SURFACE" was developed to calculate the surface coordinates and provide three-dimensional model data that can be used for finite element analysis. Development of the modeling method and an example case are presented in this report. This method of analysis could also be applied in gear inspection and near-net-shape gear forging die design.					
17. Key Words (Suggested by Author(s)) Spiral bevel gears Surface coordinates Gear geometry Finite element analysis			18. Distribution Statement Unclassified - Unlimited Subject Category 37		
19. Security Classif. (of this report) Unclassified		20. Security Classif. (of this page) Unclassified		21. No. of pages 20	22. Price* A03